Available online at www.sciencedirect.com
ScienceDirect
Nuclear Medicine and Biology 37 (2010) 965–975
NUCLEAR MEDICINE — AND — BIOLOGY
www.elsevier.com/locate/nucmedbio

In vitro and in vivo evaluation of [^{99m}Tc]-labeled tricarbonyl His-annexin A5 as an imaging agent for the detection of phosphatidylserine-expressing cells ☆

Christel Vangestel[a,*], Marc Peeters[a], Ruth Oltenfreiter[b], Yves D'Asseler[b], Steven Staelens[c], Magali Van Steenkiste[d], Jan Philippé[e], Dennis Kusters[f], Chris Reutelingsperger[f], Nancy Van Damme[a], Christophe Van de Wiele[b]

[a]*Department of Gastroenterology, Ghent University Hospital, 9000-B Ghent, Belgium*
[b]*Department of Nuclear Medicine and Radiology, Ghent University Hospital, 9000-B Ghent, Belgium*
[c]*Department of Medical Signal and Image Processing Group, Faculty of Engineering, Ghent University-IBBT, 9000-B Ghent, Belgium*
[d]*Department of Radiopharmacy, Ghent University, 9000-B Ghent, Belgium*
[e]*Department of Clinical Biology, Microbiology and Immunology, Ghent University, 9000-B Ghent, Belgium*
[f]*Department of Biochemistry, Cardiovascular Research Institute, University of Maastricht, 6200 MD Maastricht, The Netherlands*

Received 30 March 2010; received in revised form 10 May 2010; accepted 10 June 2010

Abstract

Introduction: Apoptosis is one of the mechanisms behind successful chemotherapy and radiation treatment. Radiolabeled annexin A5 has been demonstrated to be a successful tool in the detection of apoptosis following chemotherapy in vivo.
Methods: His-tagged annexin A5 was labeled with [^{99m}Tc]-tricarbonyl and evaluated as apoptosis imaging radiotracer in vitro and in vivo. The binding of the radiotracer was evaluated in Colo205 cells stimulated with 5-FU (1 mM) for 4 and 24 h, and confirmed by flow cytometry. Biodistribution and dosimetric studies were performed in healthy nude mice (n=5) via planar scintigraphy. [^{99m}Tc]-$(CO)_3$ His-annexin A5 was also evaluated for in vivo imaging of spontaneous apoptosis in Colo205-bearing mice (n=12).
Results: The labeling procedure yielded a compound with 95-99% radiochemical purity and good in vitro stability. In vitro binding experiments indicated that the radiotracer retained its PS-binding activity. [^{99m}Tc]-$(CO)_3$ His-annexin A5 rapidly cleared from the blood and predominantly accumulated in the kidneys. Absorbed dose (per organ) was found to be 116±64 μGy/MBq for the kidneys and 10.38±0.50 μGy/MBq for the liver. The effective dose was 7.00±0.28 μSv/MBq. Spontaneous apoptosis in Colo205-bearing mice was visualised by [^{99m}Tc]-$(CO)_3$ His-annexin A5 SPECT and correlated well with caspase-3 immunostaining (R=0.867, P<.01).
Conclusion: [^{99m}Tc]-$(CO)_3$ His-annexin A5 may be a useful novel radioligand for the in vivo detection of cell death associated with PS expression. A simple, noninvasive way of detecting apoptosis in vivo could have many applications including a better understanding of the extent and timing of apoptosis in response to cancer therapies and assessment of early tumor response.

Keywords: Annexin A5; Tricarbonyl; Apoptosis; Colorectal tumor model

1. Introduction

Apoptosis, or programmed cell death, is an essential process for all cellular organisms, as it is involved in both normal physiology and many disease processes including cancer development. On the one hand, cancer cells possess defective apoptotic machinery, which is one of the hallmarks of neoplastic cells, so they can continue to grow in response to growth factors. On the other hand successful chemothe-

☆ Part of this work was financially supported by the European Union through the grant Euregional PACT II by the Interreg IV program of Grensregio Vlaanderen-Nederland (IVA-VLANED-1.20).
* Corresponding author. Tel.: +32 (0)93325249; fax: +32 (0)93323807.
E-mail address: christel.vangestel@ugent.be (C. Vangestel).

0969-8051/$ – see front matter © 2010 Elsevier Inc. All rights reserved.
doi:10.1016/j.nucmedbio.2010.06.007

rapy and/or radiotherapy induces cell death, including apoptosis, in the cancer cells and indicates tumor response to therapy [1,2].

During the early phase of apoptosis, the phospholipid phosphatidylserine (PS) becomes externalized at the cell membrane. This process is one of the earliest biochemical events in the apoptotic programme. It does not depend on the apoptosis-inducing agent or cell type, persists until the apoptotic process is fully completed and promotes recognition of apoptotic cells by phagocytes or neighbouring cells [3]. The externalization of PS can be detected by using annexin A5, an endogenous human protein (36 kDa) which binds PS with nanomolar affinity (K_d=7 nM) in the presence of Ca^{2+}. Several previous reports demonstrated that fluorescent and radiolabeled annexin A5 imaging is capable of detecting and quantifying apoptosis in vivo (for review, see Ref. [4]). The most widely applied radiolabeled annexin A5 used for single positron emission computed tomography (SPECT) is the [^{99m}Tc]-hydrazinonicotinamide (Hynic)-annexin A5. [^{99m}Tc]-Hynic-annexin A5 offers a simple and fast preparation at room temperature, while providing high radiochemical yields, making this radiotracer suitable for routine production and clinical applications. However, the Hynic ligand is a bifunctional chelator capable of binding to the NH_2-terminal amino acid and lysine residues of proteins on the one hand and sequestering [^{99m}Tc] on the other hand. As any of the $-NH_2$ groups of the 21 lysines present in annexin A5 can be targeted, this labeling method is rather nonspecific. Other limitations include high uptake in the kidneys which may limit imaging in the abdominal region and may lead to high radiation burden. The persistent localization of radioactivity in the liver and kidneys is attributed to the slow elimination rate of the final radiometabolite [^{99m}Tc (Hynic-lysine)-tricine)$_2$] from the lysosymes, the main sites of intracellular catabolism of proteins. The dissociation of one of the tricine coligands at the low pH environment of the lysosymes and the absence of excess coligands lead to binding of this complex to proteins present in the organelles [5].

Hence, the demand to design suitable [^{99m}Tc]-labeled annexin A5 variants that can be used routinely and with proper apoptosis imaging qualities still remains. The [^{99m}Tc(I)]-tricarbonyl$(CO)_3$ labeling of annexin A5 via thiol functions was reported by Biechlin et al. [6] and high radiochemical yield and stabile complexes were obtained. With the use of [^{99m}Tc]-tricarbonyl core, stable complexes can also be obtained for his-tagged proteins [7]. By this labeling method, [^{99m}Tc(I)]-$(CO)_3$-labeled histidine-tagged annexin A5 may most likely retain its PS-binding affinity because site-specific labeling occurs at the N-terminal histidine tags not involved in the binding region of the protein.

The imaging of apoptosis in a noninvasive way via radiolabeled annexin A5 could be a tool to detect tumor response much earlier than other imaging techniques. Moreover, a noninvasive way to detect the extent and timing at which apoptosis occurs which is dependent on the therapeutic regimen may provide clinicians with relevant info on disease activity and therapeutic efficacy.

The main goal of this study was to characterise the radiolabeling of [^{99m}Tc]-$(CO)_3$ His-annexin A5 and to evaluate the value of this radiotracer in detecting apoptosis in vitro and in vivo in a colorectal tumor model.

2. Materials and methods

2.1. Chemicals

His-tagged annexin A5 was kindly provided by Prof. Dr. Reutelingsperger C (Department Biochemistry, University Maastricht, The Netherlands). The IsoLink kits for preparation of [^{99m}Tc]-tricarbonyl His-annexin A5 were donated by Mallinckrodt Medical BV (The Netherlands). Sephadex G-25 medium PD-10 columns were purchased from GE Healthcare Bio-Sciences AB (Uppsala, Sweden). 5-Fluorouracil was kindly provided by the Ghent University Hospital.

2.2. [^{99m}Tc]-$(CO)_3$ His-annexin A5 preparation

Preparation of the labeling precursor [^{99m}Tc]-tricarbonyl was performed according to manufacturer's instructions. Briefly, 1 ml of freshly eluted [^{99m}Tc]O_4^- (20–100 mCi, 680–3700 MBq) was added to the IsoLink vial containing the following lyophilized products: 8.5 mg sodium tartrate, 2.85 mg $Na_2B_4O_7{\cdot}10H_2O$, 7.15 mg of sodium carbonate and 4.5 mg sodium boranocarbonate. The vial was placed in a boiling water bath for 25 min. After 25 min of incubation, the tricarbonyl kit was cooled down. Four hundred microliters of the precursor was brought at pH=7 by adding stepwise 1 M HCl, and pH was checked on pH paper (Vel, Leuven, Belgium). His-annexin A5 (50–60 μg) was added to the precursor and incubated at 37°C for 1 to 1.5 h while blown dry with nitrogen gas to reduce total volume.

2.3. [^{99m}Tc]-$(CO)_3$ His-annexin A5 purification

The reaction mixture was purified on an activated Sephadex PD-10 column with phosphate-buffered saline (PBS)/0.05% bovine serum albumin (Sigma-Aldrich-Fluka, Bornem, Belgium) and eluted with fractions of 500 μl PBS.

The radioactivity of each fraction was measured in a dose calibrator (VIK-202, Veenstra, The Netherlands). High-pressure liquid chromatography (HPLC) was also performed to analyze the integrity and radiochemical purity of the radiolabeled annexin A5 with a size exclusion Shodex KW 802.5 column (7.8×300 mm; Thomsom Instrument Company) connected to a UV-VIS spectrometer (λ 280 nm, Shimadzu SPD-6AV) and a NaI γ counter (Ludlum Model 2200). Elution was performed at a flow rate of 0.8 ml/min with a 0.1 M potassium phosphate buffer (pH 7) and a Waters 510 dual-head pump. The purity of the labeled compound was furthermore analyzed with SDS-PAGE performed according to the method of Laemnli [8]. One

microcurie [^{99m}Tc]-$(CO)_3$ His-annexin A5 and 5 μg unlabeled protein were mixed with an equal volume of Laemnli sample buffer (2×) and loaded onto a 15% SDS-PAGE gel. Ten microliters of a protein ladder (10–250 kDa) from Biolabs was treated the same way. Electrophoresis was performed at 200 V until the dye front reached the bottom of the gel with a Protean III system (BioRad). Visualization of the separated proteins was done with Coomassie Brilliant Blue R-250 staining (BioRad). A super-resolution film was exposed for 1 min to the radioactive gel after which visualization of the radioactive protein was effected with Cyclone Storage Phosphor equipment (PerkinElmer, Boston, MA, USA).

2.4. Radiochemical analysis by instant thin-layer chromatography

The radiochemical purity of the [^{99m}Tc]-$(CO)_3$ His-annexin A5 was determined by ascending instant thin-layer chromatography (ITLC) with silica gel-coated fiberglass sheets (Pall Life Sciences, Pall Corporation) using physiological saline as the mobile phase. Samples of radiolabeled His-annexin A5 were tested for their in vitro stability at 4 and 24 h after preparation at 4°C and 37°C, in both PBS and RPMI cell medium supplemented with 10% fetal bovine serum (FBS). One hundred microliters of [^{99m}Tc]-$(CO)_3$ His-annexin A5 was mixed with 100 μl PBS or cell medium and incubated at 4°C and 37°C for 4 and 24 h. In vitro plasma stability experiments were also performed by combining 100 μl of human plasma and 100 μl of [^{99m}Tc]-$(CO)_3$ His-annexin and incubated at 37°C for 4 and 24 h.

ITLC was carried out with silica gel plates in 0.9% NaCl in order to define the percentage free ^{99m}Tc-pertechnetate and ^{99m}Tc-tricarbonyl. At the time points, 5 μl of the samples was spotted on TLC strips and radioactivity was counted using an automated gamma counter (Cobra II series, Canberra Packard, Meriden, CT, USA).

2.5. Colo205 cell culture

Colo205 cells, a semi-adherent human colorectal adenocarcinoma cell line (product number ATCC-CCL-222, ATCC, Manassas, VA, USA), were grown in RPMI1640 medium enriched with 10% FBS (Invitrogen, Merelbeke, Belgium) and supplemented with antibiotic–antimycotic (100×, Invitrogen) at 37°C and 5% CO_2, according to ATCC recommendations. Cells were kept in log phase by routine passage every 2–3 days (split ratio of 1:2 to 1:6).

2.6. Binding of radiolabeled annexin A5 to apoptotic cells in vitro

In order to determine whether [^{99m}Tc]-$(CO)_3$ His-annexin A5 binds to apoptotic cells in vitro, Colo205 cells were stimulated with the antimetabolite 5-fluorouracil (5-FU, pyrimidine analog) known to cause apoptosis in colorectal cancer cells. Colo205 cells were treated with vehicle or with 1 mM 5-FU for 4 and 24 h. Colo205 cells were harvested, washed two times with PBS and counted using the trypan blue method. Cells were resuspended in annexin binding buffer (Abcam, Cambridge, UK) at a final concentration of $2{\cdot}10^6$ cells/ml. Ten microcurie of [^{99m}Tc]-$(CO)_3$ His-annexin A5 was added and allowed to incubate for 30 min at room temperature. At the end of the incubation period, Colo205 cells were centrifuged (335×*g*, 5 min), supernatant was removed and cells were washed twice with annexin binding buffer. The radioactivity associated with the cell pellet was measured in an automated gamma counter (Cobra II series). Control cells were treated in a similar way. [^{99m}Tc]-$(CO)_3$ His-annexin A5 binding to cells was expressed as amount of radioactivity/$2{\cdot}10^6$ cells and compared to vehicle-treated cells. All experiments were carried out in duplicate. Induction of apoptosis in Colo205 cells by 5-FU was confirmed by flow cytometric analysis.

2.7. Flow cytometry assessment of apoptosis

Flow cytometric analyses were performed on Colo205 cells stimulated with 1 mM 5-FU for 4 and 24 h, or on control cells. $1{\cdot}10^5$ Colo205 cells were collected by centrifugation (5 min, 3000 rpm) and resuspended in 500 μl 1× annexin binding buffer. Five microliters of annexin-FITC (BioVision, Mountain View, CA, USA) and 5 μl propidium iodide (PI, BioVision) were added and incubated for 5 min in the dark. Annexin A5-FITC binding was analyzed by a Beckman Coulter Cytomics FC500 5-colour flow cytometer equipped with a 488-nm argon ion laser, using an FITC signal detector (FL1) and PI staining by the phycoerythrin emission signal detector (FL2). Viable Colo205 cells are represented by low annexin-FITC and low PI signal. Early phase apoptotic cells were identified as high annexin-FITC signal and low PI uptake, and overall dead cells (including late phase apoptotic and necrotic cells) as high or low annexin-FITC and high PI uptake.

2.8. Animal model

Female CD-1 nude mice (strain code 086) were obtained from Charles Rivers, Inc. (Wilmington, MA, USA). All mice were purchased at an age up to 42 days and were treated in accordance with Belgian regulation, and animal experiments were approved by the local ethics committee. Animals were housed in individually ventilated caging conditions under a 12-h dark/light cycle at constant humidity and temperature. Animals were permitted free access to sterile water and standard laboratory chow. For the Colo205-bearing mouse model, Colo205 cells in the log phase were harvested by trypsinization, washed three times with sterile PBS and resuspended in sterile PBS at a concentration of $1{\cdot}10^7$ per milliliter. Cells were counted using the trypan blue method. Nude mice were injected subcutaneously in the right hind leg with a suspension of $1{\cdot}10^6$ Colo205 cells in a volume of 100 μl. Tumor growth curves were obtained using calliper measurement and the

estimate volume formula V=0.4 a^2b, where a and b are the short- and long axis of the tumor, respectively. After 12–14 days of inoculation, tumors reached a volume of approximately 50–100 mm^3.

2.9. Biodistribution and dosimetry of radiolabeled annexin A5

For biodistribution and dosimetry studies, five healthy mice were anesthetized with isoflurane and the tail vein was cannulated for tracer administration. The mice were positioned in the gamma scanner and were maintained under anaesthesia for the duration of the experimental procedure, while body temperature was maintained by a heating bed. Following bolus tail-vein administration of 1 mCi [^{99m}Tc]-$(CO)_3$ His-annexin A5 in approximately 100 μl and flushing of the cannula with 100 μl saline, mice were imaged during the first 100 min (dynamic study, 10 frames of 10 min) and at 4, 8 and 22 h (planar images of 10 min) after injection of the radiotracer for evaluation of the biodistribution of [^{99m}Tc]-$(CO)_3$ His-annexin A5 in vivo. Mice were imaged with the X-SPECT system (Gamma Medica Ideas, Northridge, CA, USA) in a 10-min acquisition with the camera operated in planar mode and the animal positioned on the front plane of a small animal low-energy high-resolution collimator (hole length: 25.4 mm; septal thickness: 0.20 mm; hole diameter: 1.2 mm). Regions of interest (ROI) were drawn over the total body, liver, right kidney, left kidney, heart and part of the left hind leg (=background). ROIs were drawn on early images, and the shape and size (number of pixels) were kept constant over all subsequent images per mice. Total body retention was estimated using the no-excretion approach; that is, total counts collected during the first 10 min of the dynamic study were assumed to correspond to the total injected dose (ID). Total counts from a later whole-body scan at time t_i were used to estimate %ID according to %ID=[counts t_i/counts (first frame)×100%]. Following correction for background radiation, decay correction and checking of residual activity in the tail, uptake in the organs was expressed as percent of the injected dose.

Based upon quantification of whole-body images (0–100 min, 4 h, 8 h and 20h) from the biodistribution studies, dosimetry of [^{99m}Tc]-$(CO)_3$ His-annexin A5 was estimated using MIRDose 3.1. Organ residence time was obtained by integrating the organ activity curve that was normalised with the injected activity, but not corrected for physical decay. For liver, right kidney, left kidney and the remainder of the body, time–activity curves were constructed from the dynamic (first 100 min) and static planar scans at later time points. The data points were fitted to a mono-exponential function and the exponential function was subsequently integrated from zero to infinity to get residence times. Organ dose and effective dose were calculated with MIRDose 3.1. Data obtained from mice were converted to a 68-kg human reference adult.

2.10. In vivo imaging of spontaneous apoptosis in Colo205-bearing mice

For in vivo imaging of spontaneous apoptosis, 12 Colo205-bearing mice were injected via a tail vein with 500 μCi [^{99m}Tc]-$(CO)_3$ His-annexin A5 in 100 μl. We first verified whether there was no extravascular tail vein activity by using a human PRISM 3000XP SPECT camera operated in planar mode with each time three of these animals were anaesthetised with isoflurane and positioned on the front plane of a low-energy high-resolution collimator (±6 mm spatial resolution). Fast and short scans were acquired during 5 min with a 20% photopeak window at 140 keV. Three and a half hours postinjection (pi), mice were again brought under isoflurane anaesthesia to acquire static high-resolution tomographic images in four frames of 5 min with a focus on the tumor using the Milabs U-SPECT-II (Milabs, Utrecht, The Netherlands). This μSPECT scanner is equipped with collimators consisting of a tungsten cylinder with five rings of 15 pinhole apertures of 1.0 mm diameter delivering reconstructed images with an iteratively reconstructed resolution better than 1 mm. All pinholes focused on a single volume in the center of the tube. For this study, the animal bed was translated in three dimensions using an XYZ stage into two different bed positions focused on the tumor. A 20% main photopeak was centered at 140 keV to reconstruct the [^{99m}Tc] images on 0.75-mm^3 voxels by six iterations of 16 OSEM (ordered-subset expectation maximization) subsets. A syringe with a known amount of radioactivity was scanned along with the mice to allow semiquantification of the results using volume-of-interest (VOI) analysis. Data were expressed as %ID/tumor volume. Directly after the scan, the animals were killed by cervical dislocation and tumors were removed, formalin fixed and paraffin embedded.

2.11. Determination of apoptosis by caspase-3 immunohistochemistry

Sections of 4 μm thickness were mounted on SuperFrost microscope slides (Menzel-Glaser, Braunschweig, Germany), which were deparaffinized in xylene and rehydrated in a downgraded series of ethanol. After washing sections in dH_20, heat-induced antigen retrieval was performed for 10 min in citrate buffer (pH=6) after which the tissue slides were cooled down for 30 min. The endogenous peroxidase activity was blocked for 5 min with 0.3% hydrogen peroxide (DAKO, Glostrup, Denmark) on each tissue slide. After washing steps, each section was blocked with a blocking solution (TBST/5% normal goat serum) for 1 h at room temperature. Primary antibody Cleaved Caspase-3 (Cell Signaling Technology, #9661, 1/400 dilution in PBST/5% normal goat serum) was then incubated overnight at 4°C. After washing, the tissue sections were incubated for 30 min at room temperature with a labeled polymer-HRP anti-rabbit secondary antibody (DAKO). The colour reaction was developed using the

chromogen 3,3-diaminobenzidine+ (DAB) for 10 min. After washing, the tissue sections were counterstained with Mayer's haematoxylin. TBST/5% normal goat serum instead of the primary antibody was used as negative control in order to exclude false-positive responses from nonspecific binding of the secondary antibody. Prior to staining of the specimens, an isotype control was performed to estimate the nonspecific binding of target primary antibodies to cell surface antigens.

The number of apoptotic cell fragments present in each tumor specimen was expressed as a fraction of the total number of cells. The apoptotic index was determined by Optronics Color digital camera (Olympus Corporation, Tokyo, Japan) and specialized software (Cell D Olympus Imaging Solutions, Münster, Germany). Ten ROIs were chosen at random at a magnification of 200×. High necrotic regions were excluded for analysis.

2.12. Statistical analysis

All statistical analysis was performed using SPSS software (version 15.0; SPSS, Inc., Chicago, IL, USA). Data are expressed as mean±S.D. When statistical significance was tested between two groups, data were subjected to the Mann–Whitney test (independent samples). Spearman correlation was used to calculate correlations between [^{99m}Tc]-$(CO)_3$ His-annexin A5 tumor uptake and caspase-3-positive cells in the tumor. Data were considered statistically significant when a two-tailed P value of <.05 was reached.

3. Results

3.1. Radiochemical profile of [^{99m}Tc]-$(CO)_3$ His-annexin A5

His-tagged annexin A5, with an N-terminal extension containing six histidine residues, was successfully labeled with [^{99m}Tc]-$(CO)_3$. Incubation of the His-annexin A5 with the [^{99m}Tc]-$(CO)_3$ occurred at physiological pH (pH=7) and at 37°C for about 1- 1.5h. Radiochemical yields of 70-85% and specific radioactivities of approximately 140-160 μCi/μg protein were obtained. Before animal administration, [^{99m}Tc]-$(CO)_3$ His-annexin A5 was purified on a PD-10 gel permeation column using PBS as eluent. The radiochemical purity of the labeled annexin A5 was evaluated by ITLC with physiological saline as mobile phase. Radiochemical purities of 95–99% were obtained with the remainder being free [^{99m}Tc] pertechnetate (1–5%). HPLC was performed to characterize the radiolabeled His-annexin A5. [^{99m}Tc]-$(CO)_3$ His-annexin A5 complex was eluted at a retention time of 9.8 min. One small peak (5%) before the actual [^{99m}Tc]-$(CO)_3$ His-annexin A5 peak was observed, which may present dimers of annexin A5. The SDS-PAGE showed a band of 36 kDa representing the labeled His-annexin A5 and a smaller higher band representing the annexin A5 dimers (Fig. 1). No other small molecules were identified.

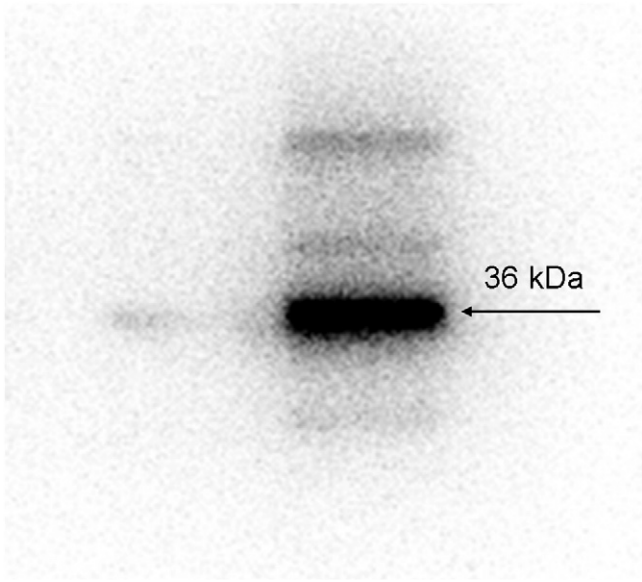

Fig. 1. SDS-PAGE of radiolabeled [^{99m}Tc]-$(CO)_3$ His-annexin A5. The radiolabeled His-annexin A5 has a molecular weight of 36 kDa, as indicated by the arrow. Small higher bands are visible, probably representing annexin A5 dimers.

In vitro, no significant degradation of the product was noted for up to 24 h, at 4°C and 37°C in saline or in cell media supplemented with 10% FBS. The stability tests demonstrated that [^{99m}Tc]-$(CO)_3$ His-annexin A5 has good thermodynamic stability in saline and in cell media/10% FBS. The stability of [^{99m}Tc]-$(CO)_3$ His-annexin A5 was also checked in human plasma at 37°C. Less than 1% of the total radioactivity was detected by ITLC after 4 h of incubation as free pertechnetate, indicating good stability of the labeled complex after 4 h. After 24 h of incubation, 15% of the total radioactivity was detected as free pertechnetate, indicating that some degradation of the radiotracer has occurred.

3.2. Binding of radiolabeled annexin A5 to apoptotic cells in vitro

In order to determine whether His-annexin A5 maintained its biological activity after labeling with [^{99m}Tc]-$(CO)_3$, binding studies with Colo205 stimulated with 5-FU were performed. After 4 h of incubation of Colo205 cells with 5-FU, the binding of [^{99m}Tc]-$(CO)_3$ His-annexin A5 to 5-FU treated cells is significantly higher (37.5% increase) than binding to vehicle-treated cells (P=.021). 5-FU-treated Colo205 cells for 24 h showed a 106% increase in the binding of [^{99m}Tc]-$(CO)_3$ His-annexin A5, compared to control cells (P=.0286; Fig. 2). However, a relatively high binding of the radiotracer to untreated cells was also observed, which may be due to nonspecific sticking of the labeled annexin A5 to the wall of the tubes, or it may indicate a high rate of spontaneous apoptosis in the Colo205 cells.

The apoptotic cell fractions (measured by flow cytometry based on annexin A5-FITC and PI staining) of Colo205 cells

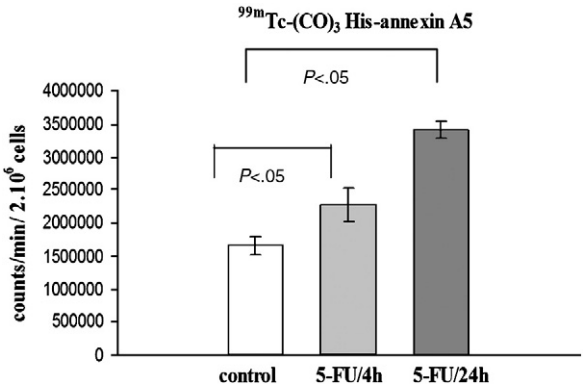

Fig. 2. Binding of [^{99m}Tc]-$(CO)_3$ His-annexin A5 to Colo205 cells, incubated for 4 and 24 h with vehicle (control) or 5-FU (1 mM). A significant increase in [^{99m}Tc]-$(CO)_3$ His-annexin A5 binding to 5-FU-stimulated Colo205 for 4 h (P=.021) and for 24 h (P=.0286) vs. control cells was demonstrated. The coloured bars represent the means of five experiments and error bars refer to the standard deviation of the means.

receiving vehicle or 5-FU for 4 and 24 h are shown in Fig. 3. In control Colo205 cells, a small fraction of spontaneous apoptotic cells was observed (2.9±0.66% early phase apoptotic, 2.71±0.32% late phase apoptotic+necrotic cells). Colo205 cells stimulated for 4 h with 1 mM 5-FU showed a small increase of early phase apoptotic cells (3.23±0.21%) but particularly a higher increase (P=.05) in the late phase apoptotic+necrotic cells (7.03±0.32%). Incubation of Colo205 cells for 24 h with 1 mM 5-FU led to an overall increase of apoptotic cells compared to control cells [17.75±0.35% early phase apoptotic cells (P=.05) and 6.3±0.42% late phase apoptotic+necrotic cells (P=.05)].

3.3. Biodistribution

Five healthy mice received intravenous injection of the radiotracer (1 mCi) and were imaged during the first 100 min (dynamic) and at 4, 8 and 22 h pi. The biodistribution of radioactivity following injection of [^{99m}Tc]-$(CO)_3$ His-annexin A5 in nude mice is summarized in Table 1. Following intravenous injection of [^{99m}Tc]-$(CO)_3$ His-annexin A5, the radiotracer was rapidly cleared from the blood (7.02±0.44 %ID during the first 10 min and at 1 h pi only 1.39±0.13 %ID remained in the blood; Fig. 4).

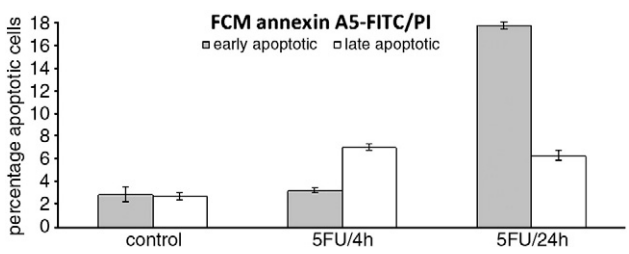

Fig. 3. Flow cytometric results for Colo205 cells after incubation with the vehicle 5-FU (1 mM) for 4 and 24 h. With the use of annexin-V FITC and PI stain, an increase in apoptotic cell fraction was observed after stimulation of Colo205 cells with 5-FU for 4 and 24 h. Control Colo205 cells showed only a low level of spontaneous apoptosis.

Table 1
Biodistribution studies of [^{99m}Tc]-(CO)3 His-annexin A5 in nude mice, expressed as %ID

Time postinjection (min)	Blood (n=5)	Right kidney (n=5)	Left kidney (n=5)	Liver (n=5)
10	7.02±0.44	18.60±1.93	13.41±1.14	13.41±1.41
20	4.26±0.93	26.05±2.49	22.06±1.59	11.74±2.80
30	2.42±0.34	28.75±2.14	24.63±1.46	8.87±0.27
40	1.81±0.24	29.05±1.96	25.38±1.47	8.74±0.23
50	1.55±0.15	28.75±1.77	25.01±1.67	8.87±0.27
60	1.39±0.13	28.41±1.77	24.58±1.53	9.02±0.31
70	1.28±0.10	27.95±1.81	24.08±1.57	9.14±0.31
80	1.23±0.11	27.35±1.75	23.75±1.64	9.28±0.27
90	1.13±0.09	26.88±1.67	23.30±1.71	9.23±0.65
100	0.99±0.21	26.37±1.60	22.69±1.81	9.11±0.99
240	0.21±0.31	18.75±3.08	15.63±2.42	5.83±1.26
480	0.05±0.24	13.84±1.31	11.69±1.15	5.24±0.73
1320	0.11±0.09	8.39±0.56	6.62±0.59	2.78±0.42

The kidneys had the highest concentration throughout the entire length of the experiment. The right kidney showed a higher uptake of the radiotracer compared to the left kidney at all time points. Analysis of biodistribution data demonstrated that particularly the renal cortex had a high uptake of the radiotracer. The organ with the second highest radioactivity was the liver and there was little overall change in its biodistribution during the first 100 min pi (13.41±1.41 %ID during the first 10 min and 9.11±0.99 %ID at 100 min pi). Total body activity remained constant during the first 100-min dynamic imaging and gradually decreased at 4 h (60% of initial total body±4.92), 8 h (52±0.39%) and 22 h pi (30.52±0.19%). The biological half-life in the total body is approximately 5.5 h.

No activity in the thyroid and in the stomach was visible, confirming the absence of free pertechnetate in the injectate (already confirmed by ITLC) and confirming the substantial stability of the [^{99m}Tc]-$(CO)_3$ His-annexin A5 complex in vivo.

So for [^{99m}Tc]-$(CO)_3$ His-annexin A5, renal excretion is the predominant route of clearance, with a lower uptake in the hepatic region, while no uptake could be visually observed in the gastrointestinal region (Fig. 5).

3.4. Dosimetry

To translate the biodistribution data in mice into estimates of patient dose, the organ values were extrapolated from the data derived from the biodistribution data of a 68-kg man using the standard MIRD scheme and S tables. A summary of dosimetric parameters for the main organs and total body is given in Table 2. The percentage uptake for the organs is shown at 1 h after intravenous injection. Kidneys clearly had the highest uptake and the highest absorbed dose, followed by the liver. The effective dose equivalent (EDE) and the

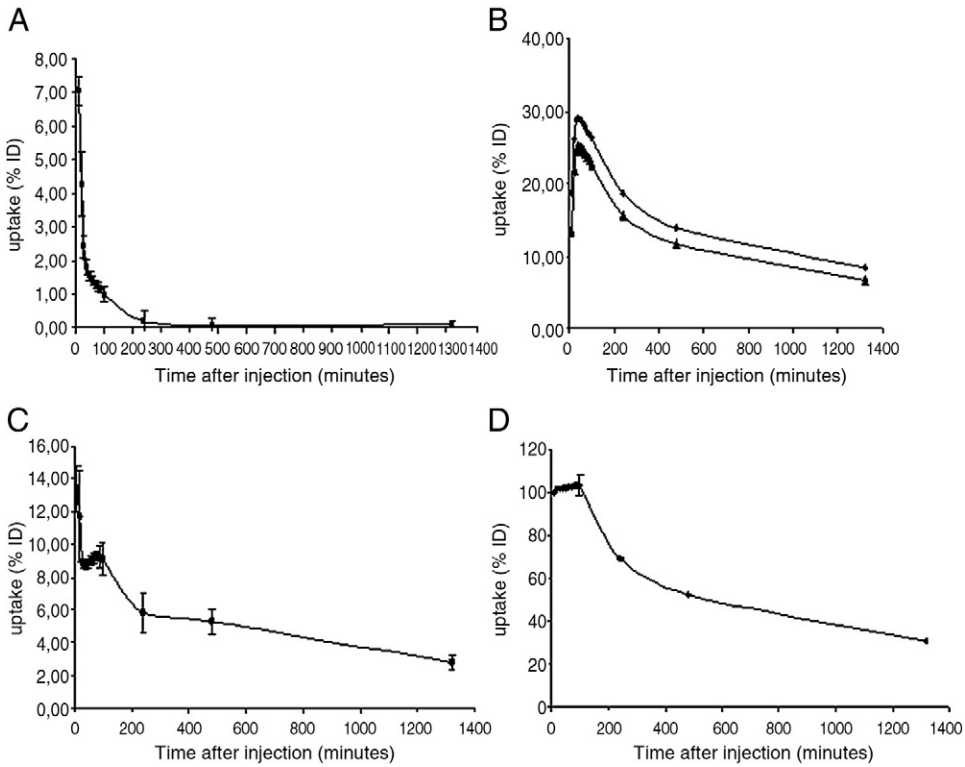

Fig. 4. Decay-corrected [^{99m}Tc]-(CO)$_3$ His-annexin A5 uptake vs. time curves for (A) blood pool; (B) (♦) curves represent right kidney, (▲) represent left kidney; (C) liver and (D) total body. Planar, dynamic scans were made from 0 to 100 min (10 frames of 10 min), and planar images were obtained at 4, 8 and 22 h pi (10 min acquisition time). Kidneys were the main organs of radiotracer uptake (higher in the right kidney than in the left kidney), followed by the liver. A rapid clearance of the tracer from the blood was observed.

effective dose (ED) were calculated to be 12.7±0.68 and 7.00±0.28 μSv/MBq, respectively. The EDE and the ED, when calculations were made per gram of tissue, were 5.71±0.27 and 3.64±0.04 μSv/MBq, respectively.

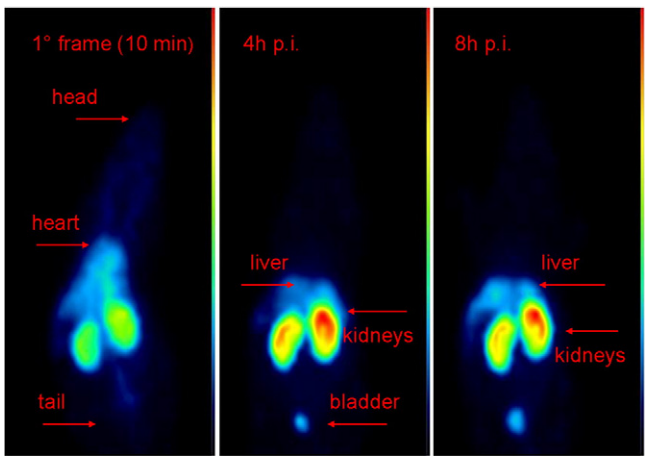

Fig. 5. Posterior view of scintigraphic images showing in vivo biodistribution of [^{99m}Tc]-(CO)$_3$ His-annexin A5 in a healthy mice under isoflurane anaesthesia after administration of [^{99m}Tc]-(CO)$_3$ His-annexin A5 (1 mCi), during the first 10 min, 4 and 8 h after injection of the radiotracer (acquisition time of 10 min). Rapid clearance from the blood is demonstrated. Kidneys are the main organs of radiotracer uptake, followed by the liver.

The total ED for a proposed single injection of a dosage of 500 MBq (13.5 mCi) [^{99m}Tc]-(CO)$_3$ His-annexin A5 will be 3.5±0.14 mSv (ED per organ) or 1.82±0.02 mSv (ED per gram of organ). MIRDose 3.1 also gives estimates of the dose in other organs, for example, the absorbed dose (per organ) for the lungs, ovaries, testes and uterus (radiation-sensitive organs) is 2.41±0.02, 2.52±0.06, 1.25±0.08 and 2.46±0.04 μGy/MBq, respectively (per organ).

3.5. In vivo imaging of spontaneous apoptosis in Colo205-bearing mice

After successful labeling of His-tagged annexin A5 with [^{99m}Tc], its characterization and biodistribution profile, its imaging efficacy in an in vivo system was explored. Untreated mice with subcutaneous Colo205 tumors in the hind leg were used to visualize spontaneous apoptosis by [^{99m}Tc]-(CO)$_3$ His-annexin A5 SPECT scans. Colo205-bearing mice were intravenously injected with 500 μCi of [^{99m}Tc]-(CO)$_3$ His-annexin A5 in a lateral tail vein. Three and a half hours postinjection of the radiotracer, mice were sedated with isoflurane inhalation, while body temperature was maintained constant and tomographic images with a resolution better than 1 mm of the mice (focused on the tumor) were made using the

Table 2
Dosimetric data for intravenously administered [^{99m}Tc]-(CO)3 His-annexin A5

Site	Uptake[a] (%ID)	Per organ		Per gram of tissue	
		Residence time (h)	Absorbed dose (μGy/MBq)	Residence time (h)	Absorbed dose (μGy/MBq)
Right kidney	28.41±1.77	1.61±0.13	116±64	0.65±0.06	56.94±3.84
Left kidney	24.58±1.53	1.35±0.09	116±64	0.49±0.04	56.94±3.84
Liver	9.02±1.53	0.57±0.04	10.38±0.59	0.21±0.02	4.29±0.18
Remainder	–	2.52±0.17	–	2.71±0.19	–
Total body	100	6.07±0.06	12.72±0.68[b] 7.00±0.28[c]	6.07±0.06	5.71±0.27[b] 3.64±0.04[c]

Data are mean±SD (n=5).
[a] Uptake values (%ID) obtained 1 h pi and were corrected for physical decay.
[b] Effective dose equivalent in microsievert per megabecquerel.
[c] Effective dose in microsievert per megabecquerel.

U-SPECT-II. All tumors were visually detectable and showed a heterogeneous uptake of the radiotracer. Radiotracer uptake in the tumors was calculated by VOI analysis, which resulted in a mean uptake of 0.2574±0.0614 %ID/tumor volume. Verification for extravascular tail vein activity was verified by whole-body planar scans using a human SPECT PRISM 3000XP scanner.

Ex vivo immunohistochemical staining of caspase-3 of the tumor slides (Fig. 6) revealed a mean percentage of apoptotic cells of 1.3960±0.4031 and correlated well with [^{99m}Tc]-(CO)$_3$ His-annexin A5 uptake (R=0.867, P<.01; Fig. 7A and B).

4. Discussion

The hallmark for the start of apoptosis is the redistribution and exposure of the anionic phospholipid PS on the cell surface. PS is normally restricted to the inner leaflet of the cell membrane, but becomes rapidly exposed to the outer leaflet of the cell membrane in response to apoptotic signals [3]. PS therefore represents an ideal target for the detection of apoptotic cell bodies, in vitro as well as in vivo. The most widely used method for the detection of apoptotic bodies involves the use of fluorescent or radiolabeled annexin A5, known for its high affinity for cell membrane-bound PS [9]. The goal of this study was to synthesize and characterize [^{99m}Tc]-(CO)$_3$ His-annexin A5 as a potential tool for the noninvasive imaging of cell death accompanied by PS exposure, including apoptosis.

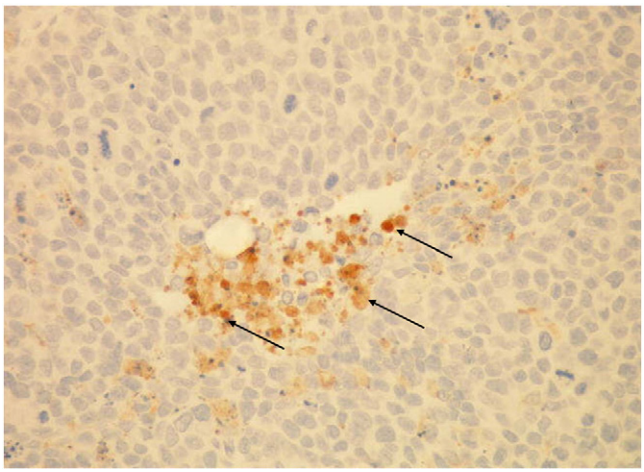

Fig. 6. Caspase-3 immunohistochemical staining of dissected Colo205 tumors (200×). Black arrows indicate caspase-3-positive cells representing spontaneous apoptotic cell bodies in untreated Colo205 tumors.

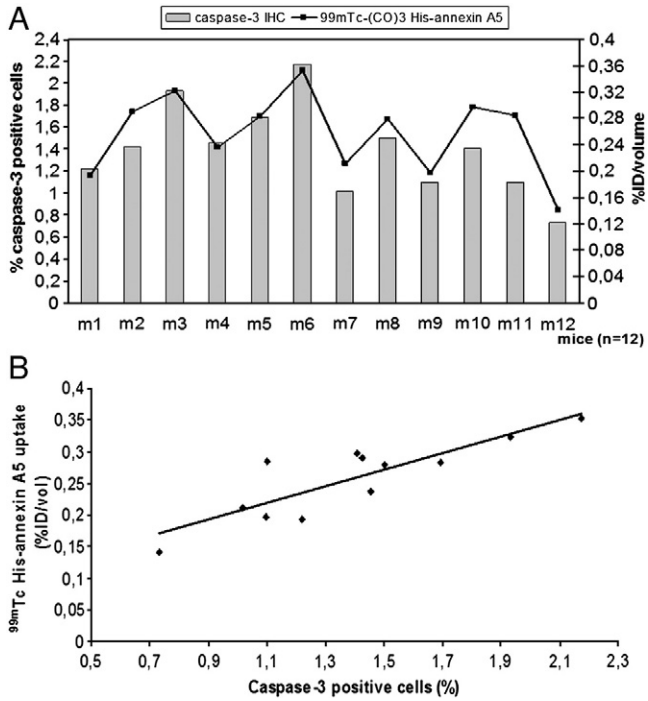

Fig. 7. (A) [^{99m}Tc]-(CO)$_3$ His-annexin A5 tumor uptake in all 12 mice is demonstrated, together with percentage of caspase-3-positive cells. [^{99m}Tc]-(CO)$_3$ His-annexin A5 uptake is expressed as %ID/tumor volume. (B) Correlation of [^{99m}Tc]-(CO)$_3$ His-annexin A5 uptake and caspase-3-positive cells in Colo205 tumors. Tumor uptake of [^{99m}Tc]-(CO)$_3$ His-annexin A5 significantly correlated with percentage of caspase-3-positive cells in tumor (R=0.867, P<.01).

His-tagged annexin A5 was successfully labeled with [^{99m}Tc]-$(CO)_3$, with yields of approximately 70–85% and high radiochemical purities (≥95%). The incubation of the annexin A5 protein with the [^{99m}Tc]-tricarbonyl occurs at 37°C and at physiological pH, which are optimal conditions for the annexin A5, a protein of which the phospholipid-binding activity becomes rapidly destroyed by heating [10]. The radiotracer remained stable for up to 24 h, at 4°C and 37°C, in physiological solution and cell media/10% FBS, demonstrating a good stability of the compound.

In vitro binding characteristics proved that [^{99m}Tc]-$(CO)_3$ His-annexin A5 retained its PS-binding capacity. Colo205 cells were incubated for 4 and 24 h with the pyrimidine analog 5-FU to induce apoptosis. Its active metabolite 5-fluoro-2′-deoxyuridine-5′-monophosphate inhibits thymidylate synthase and causes thymine depletion and subsequent cell-cycle arrest and apoptosis in human colon cancer cell lines [11]. Colo205 cells stimulated for 4 and 24 h with 5-FU demonstrated a significantly higher uptake of [^{99m}Tc]-$(CO)_3$ His-annexin A5 (37.5% and 106%, respectively) compared to control cells. Flow cytometric analysis of 5-FU-stimulated Colo205 cells for 4 and 24 h was performed with annexin-FITC and PI staining, and demonstrated a gradual increase in apoptotic/necrotic cells compared to nonstimulated control cells. After 4 h of incubation with 5-FU, late phase apoptotic cells+necrotic cells increased to 7.02% compared to control cells (2.71%), and after 24 h of incubation, early phase apoptotic cells increased to 17.75% compared to control cells (2.9%) and late phase apoptotic cells+necrotic cells increased to 6.3% compared to control cells. The low percentage of apoptotic +necrotic cells observed in the control cells by flow cytometry shows a low level of spontaneous apoptosis, indicating that the high uptake of the radiolabeled annexin A5 by the control cells is due to nonspecific sticking to the wall rather than presenting high levels of spontaneous apoptosis. The flow cytometric results confirmed the in vitro results with the radiolabeled annexin A5 binding to either apoptotic or necrotic cells. More extensive experiments are required to measure the actual PS affinity of this radiotracer; however, this was beyond the scope of the current study.

It is generally accepted that fluorescent or radiolabeled annexin A5 is an apoptosis-detecting probe; however, apoptosis is not the sole cell death type which is accompanied by PS expression. During the necrotic process, PS binding sites may become accessible for the annexin A5, and other types of cell death are also accompanied by externalization of PS including autophagy, anoikis and mitotic catastrophe [12,13]. So by no means do annexin A5-based probes exclusively detect apoptotic events. However, a rather overall cell death (in fact, cell death accompanied by PS expression) is detected when using annexin A5-based probes [14].

Following intravenous injection, [^{99m}Tc]-$(CO)_3$ His-annexin A5 rapidly clears from the blood. The biodistribution study performed in nude mice demonstrated a predominant uptake of the radiotracer in the kidneys, followed by the liver, indicating a urinary excretory pathway of the tracer. Uptake in the right kidney was higher than in the left kidney at all time points, which may be explained by a partial overlap of the right kidney with the liver. High accumulation of the radiotracer in the renal cortex may be attributed to high concentrations of PS in that region or to the nonspecific uptake of low-molecular-weight proteins by proximal renal tubule cells, as previously described [15,16]. The biodistribution did not reveal any substantial bowel excretion, resulting in good imaging conditions in the abdominal region; this is in contrast to other [^{99m}Tc]-labeled annexin A5 variants such as [^{99m}Tc]-BTAP-annexin A5 and [^{99m}Tc]-labeled annexin A5 in the presence of SDH, PDTA, tricine and nicotinic acid [17,18]. Overall, the pharmacokinetics of [^{99m}Tc]-$(CO)_3$ His-annexin A5 are somewhat similar to those of [^{99m}Tc]-Hynic-annexin A5 in mice, rats, rabbits and swine [19-21]. However, for [^{99m}Tc]-Hynic-annexin A5, other organs that have concentrated radiolabeled annexin A5 include the spleen, bone marrow, stomach and lungs [19,20]. For [^{99m}Tc]-$(CO)_3$ His-annexin A5, these organs did not show visible uptake. The biological half-life of [^{99m}Tc]-$(CO)_3$ His-annexin A5 determined in nude mice is approx. 5.5 h, which is shorter than the biological half-lives of [^{99m}Tc]-Hynic-annexin A5 (69±7 h), [^{99m}Tc]-BTAP-annexin A5 (16±7 h) and [^{99m}Tc]-i-annexin A5 (62±13 h) determined in humans [17,22,23]. The faster clearance of the [^{99m}Tc]-$(CO)_3$ His-annexin A5 may result in lower background activity; however, it may also lead to a smaller probability of binding of the radiotracer to the PS-binding sites in vivo.

As previously mentioned, the [^{99m}Tc(I)]-$(CO)_3$-labeled histidine-tagged annexin A5 most likely retains its PS-binding affinity because site-specific labeling occurs at the N-terminal histidine tags not involved in the binding region of the protein. Recently, an annexin A5 conjugate has been developed with a cysteine residue at its concave site, the so-called second-generation annexin A5. In this way, the used chelator is located at a well-defined position outside the binding region of the protein, thus not affecting the PS binding properties. This novel [^{99m}Tc]-Hynic-cys-annexin A5 had a similar biodistribution pattern as the first-generation [^{99m}Tc]-Hynic-annexin A5 [24,25]. In a recent study, the second-generation annexin A5 was labeled in three different ways (Hynic, DTPA, and tricarbonyl-His-tagged cys-annexin A5). A faster urinary excretion was shown for the tricarbonyl His-cys-annexin A5 compared to the other two, and hepatobilliary excretion was found for all three. After 4 h, [^{99m}Tc]-Hynic-cys annexin A5 uptake in the liver was significantly lower than the other two. Blood clearance was fastest for [^{99m}Tc]-Hynic-cys annexin A5, while the other two remained longer in the blood [26].

Application of [^{99m}Tc]-$(CO)_3$ His-annexin A5 to patients would cause an effective dose of 7.00±0.28 μSv/MBq

corresponding to a total effective dose of 3.5±0.14 (ED per organ) mSv for a patient dose of 500 MBq. These values are in the low range compared to those for [^{99m}Tc]-i-annexin A5 (9.7 μSv/MBq), [^{99m}Tc]-BTAP-annexin A5 (7.6 μSv/MBq) and [^{99m}Tc]-Hynic-annexin A5 (11 μSv/MBq) [17,23,24]. However, allometric scaling from the laboratory animals to humans was performed on the basis of body/organ weight which assumes that the biokinetics of compounds mainly depend on the metabolic rate of the animal which in turn is a function of the body weight or body surface area. The effective dose obtained in this study gives only an idea of the possible effective dose that would be obtained in human patients. A detailed study in humans for a reliable estimate of the effective dose, however, is still recommended.

To image spontaneous levels of apoptosis in vivo, Colo205-bearing mice were imaged on the U-SPECT-II (tomographic, acquisition time of 20 min) 3.5 h after injection of 500 μCi [^{99m}Tc]-$(CO)_3$ His-annexin A5 to allow sufficient blood pool clearance. A heterogeneous uptake of the radiotracer was seen in all tumors corresponding to a heterogeneous distribution of spontaneous apoptosis. A high and significant correlation between [^{99m}Tc]-$(CO)_3$ His-annexin A5 uptake and number of caspase-3-positive cells was demonstrated. Externalization of PS immediately follows caspase-3 activation in the early phase of the apoptotic process, so both apoptotic markers are closely time related. This is in contrast to the widely used apoptotic marker, terminal deoxynucleotidyl transferase-mediated deoxyuridine triphosphate nick-end labeling, which detects DNA degradation occurring in the late phase of the apoptotic programme.

5. Conclusion

His-tagged annexin A5 was successfully labeled with [^{99m}Tc]-$(CO)_3$. Biodistribution study demonstrated that the main excretion routes are via the kidneys and liver, while other organs showed little or no visible uptake. The effective dose of 3. 64 μSv/MBq (per gram of tissue) is in the lower range of values found for [^{99m}Tc]-labeled annexin A5 compounds. Spontaneous apoptosis in Colo205-bearing mice was visualised with the radiotracer and correlated well with ex vivo immunohistochemical staining of caspase-3. The favourable biodistribution, the low effective dose and the ability to image apoptosis in vivo in tumor-bearing mice make this radiotracer a promising candidate for the use in clinical practice for, e.g., early assessment of tumor response in cancer patients.

Acknowledgments

We would like to acknowledge Covidien for kindly providing us with the IsoLink kits. We would also like to express our gratitude to P. Joye for his excellent assistance in animal handling and S. Deleye for his technical assistance in handling the U-SPECT-II. We are indebted to Dr. K. Bachert for his assistance in dosimetric analysis.

References

[1] Gerl R, Vaux DL. Apoptosis in the development and treatment of cancer. Carcinogenesis 2005;26:263–70.
[2] de Bruin EC, Medema JP. Apoptosis and non-apoptotic deaths in cancer development and treatment response. Can Treatment Rev 2008; 34:737–49.
[3] Zwaal RFA, Comfurius P, Bevers EM. Surface exposure of phosphatidylserine in pathological cells. Cell Mol Life Sci 2005;62: 971–88.
[4] Blankenberg FG. In vivo detection of apoptosis. J Nucl Med 2008;49: 81S–95S.
[5] Ono M, Arana Y, Uehara T, Fujiaka Y, Ogawa K, Namba S, et al. Intracellular metabolic fate of radioactivity after injection of technetium-99m-labeled hydrazine nicotinamide derivatized proteins. Bioconjug Chem 1999;10:386–94.
[6] Biechlin ML, Bonmartin A, Gilly FN, Fraysse M, du Moulinet d'Hardemare A. Radiolabeling of annexin A5 with ^{99m}Tc: comparison of Hynic-Tc vs. iminothialane-Tc-tricarbonyl conjugates. Nucl Med Biol 2008;35:679–87.
[7] Waibel R, Alberto R, Willuda J, Finnern R, Schibli R, Stichelberger A, et al. Stable one-step technetium-99m labeling of His-tagged recombinant proteins with a novel Tc(I)-carbonyl complex. Nature Biotech 1999;17:897–901.
[8] Laemnli UK. Cleavage of structural proteins during the assembly of the head of bacteriophage T4. Nature 1970;227:680–5.
[9] Koopman G, Reutelingsperger CP, Kuijten GA, Keehnen RM, Pals ST, van Oers MH. Annexin V for flow cytometric detection of phosphatidylserine expression on B cells undergoing apoptosis. Blood 1994;84:1415–20.
[10] Reutelingsperger CPM, Hornstra G, Hemker HC. Isolation and partial purification of a novel anticoagulant from arteries of human umbilical cord. Eur J Biochem 1985;151:525–9.
[11] Tillman DM, Petak I, Houghton JA. A Fas-dependent component in 5-fluorouracil/leucovorin-induced cytotoxicity in colon carcinoma cells. Clin Can Res 1999;5:425–30.
[12] Brouckaert G, Kalai M, Krysko DV, Saelens X, Vercammen D, Ndlovu M, et al. Phagocytosis of necrotic cells by macrophages is phosphatidylserine dependent and does not induce inflammatory cytokine production. Mol Biol Cell 2004;5:1089–100.
[13] Eom YW, Kim MA, Park SS, Goo MJ, Kwon HJ, et al. Two distinct modes of cell death induced by doxorubicin: apoptosis and cell death through mitotic catastrophe accompanied by senescence-like phenotype. Oncogene 2005;24:4765–77.
[14] Corsten MF, Hofstra L, Narula J, Reutelingsperger CPM. Counting heads in the war against cancer: defining the role of annexin A5 imaging in cancer treatment and surveillance. Cancer Res 2006;66: 1255–60.
[15] Sterin-Speziale N, Kahane VL, Setton CP, Fernandez MC, Speziale EH. Compartmental study of the rat renal phospholipids metabolism. Lipids 1992;27:10–4.
[16] Lang L, Jagoda E, Wu CH. Factors influencing the in vivo pharmacokinetics of peptides and antibody fragments: the pharmacokinetics of two PET-labeled low molecular weights proteins. Q J Nucl Med 1997;41:53–61.
[17] Kemerink GJ, Boersma HH, Thimister PWL, Hofstra L, Liem IH, Pakbiers MTW, et al. Biodistribution and dosimetry of ^{99m}Tc-BTAP-annexin A5 in humans. Eur J Nucl Med 2001;28:1373–8.
[18] Subbarayan M, Häfeli UO, Feyes DK, Unnithan J, Emancipator SN, Mukhtar H. A simplified method for preparation of ^{99m}Tc-annexin V and its biological evaluation for in vivo imaging of apoptosis after photodynamic therapy. J Nucl Med 2003;44:650–6.

[19] Blankenberg FG, Katsikis PD, Tait JF, Davis E, Naumovski L, Ohtsuki K, et al. Imaging of apoptosis (programmed cell death) with ^{99m}Tc annexin V. J Nucl Med 1999;40:184–91.

[20] Ohtsuki K, Akashi K, Aoka Y, Blankenberg FG, Kopiwoda S, Tait JF, et al. Technetium-99mHYNIC-annexin V: a potential for the in-vivo detection of apoptosis. J Eur J Nucl Med 1999;26: 1251–8.

[21] Tait F, Cerqueira MD, Dewurst TA, Fuijika K, Ritchie JL, Stratton JR. Evaluation of annexin V as a platelet-directed thrombus targeting agent. Thromb Res 1994;75:491–501.

[22] Kemerink GJ, Liu X, Kieffer D, Ceyssens S, Mortelmans L, Verbruggen A, et al. Safety, biodistribution, and dosimetry of ^{99m}Tc-HYNIC-annexin V, a novel human recombinant annexin V for human application. J Nucl Med 2003;44:947–52.

[23] Kemerink GJ, Liem IH, Hofstra L, Boersma hH, Buijs WCAM, Reutelingsperger CPM, et al. Patient dosimetry of intravenously administered ^{99m}Tc-annexin V. J Nucl Med 2001;42:382–7.

[24] Greupink R, Sio CF, Ederveen A, Orsel J. Evaluation of a ^{99m}Tc-labeled annexin A5 variant for non-invasive SPECT imaging of cell death in liver, spleen and prostate. Pharm Res 2009;26:2647–56.

[25] Fonge H, de Saint Hubert M, Vunckx K, Rattat D, Nuyts J, Bormans G. Preliminary in vivo evaluation of a novel ^{99m}Tc-labeled HYNIC-cys-annexin A5 as an apoptosis imaging agent. Bioorg Med Chem Lett 2008;18:3794–8.

[26] De Saint-Hubert M, Mottaghy FM, Vunckx K, Nuyts J, Fonge H, Prinsen K. Site-specific labeling of 'second generation annexin V with $^{99m}Tc(CO)_3$ for improved imaging of apoptosis in vivo. Bioorg Med Chem 2010;18:1356–63.